*Supported in part by the National Science Foundation.

†Present address: Physics Department, New York University, 4 Washington Place, New York, N. Y. 10003.

[1]J. Macek and R. Shakeshaft, Phys. Rev. Lett. **27**, 1487 (1971); R. Shakeshaft and J. Macek, Phys. Rev. A **6**, 1876 (1972).

[2]H. S. W. Massey and E. H. S. Burhop, *Electronic and Ionic Impact Phenomena* (Oxford, U. P., New York, 1952), p. 450.

[3]L. Wilets and S. J. Wallace, Phys. Rev. **169**, 84 (1968).

[4]F. Herman and S. Skillman, *Atomic Structure Calculations* (Prentice-Hall, Englewood Cliffs, N. J., 1963).

[5]D. W. Koopman, Phys. Rev. **154**, 79 (1967).

[6]It was incorrectly stated in the second paper of Ref. 1 that $P_s^{\max}$ decreases with energy. It is, in fact, the value of P_s at large ρ which decreases with energy. In the same paper we quoted the value 0.30 for $P_s^{\max}$ at 1 keV. This value was obtained from two-state calculations which are quite inadequate at such high energies.

[7]W. Lindstrom, R. Garrett, and U. Von Mollendorff, Nucl. Instru. Methods **93**, 385 (1971).

PHYSICAL REVIEW A VOLUME 7, NUMBER 5 MAY 1973

Angular Distribution in the Two-Quantum Atomic Photoeffect

E. Arnous, S. Klarsfeld, and S. Wane

Institut de Physique Nucléaire, Division de Physique Théorique , 91406 Orsay-France*

(Received 27 November 1972)

Total and differential two-photon ionization cross sections are derived in the framework of perturbation theory, assuming a simple one-electron atomic model. It is shown that for an unpolarized target the angular distribution of the ejected electrons has the general form $a+b\cos^2\theta+c\cos^4\theta$, whatever the quantum numbers n, l, of the initial energy level, and the state of polarization (linear or circular) of the incident radiation. The total transition rates for circularly and for linearly polarized light are quite different from each other. For an arbitrary nl state, the theoretically allowed maximum value of their ratio is 3/2. Further analytical and numerical results are presented for hydrogen. The Appendix contains several useful summation formulas for spherical harmonics.

I. INTRODUCTION

Recent progress in lasers and electron detection techniques makes it possible to design experiments in which one measures not only total but also differential cross sections of photoionization and photodetachment processes. The ejection of an outer electron may be consecutive to the absorption of one or more photons from the incident beam. With presently available lasers the first case occurs only in negative ions, owing to the weak binding of the additional electron, whereas photoionization of neutral atoms will generally be a multiphoton (i.e., a higher-order) process.

For linearly polarized radiation and an unpolarized target the angular distribution of electrons emitted in one-photon dipole transitions can be shown to have the universal form $a+b\cos^2\theta$. The coefficients a and b depend on the photon energy and on the quantum numbers of the initial atomic state, and θ is the angle between the momentum of the ejected electron and the photon polarization. This simple form follows from general symmetry considerations and holds as well for one-electron as for many-electron atoms and even for molecules.[1] A detailed review of this subject has been given recently by Cooper and Zare.[2] They also briefly discussed the two-photon ionization process in the framework of perturbation theory, and showed that the electron angular distribution still retains a simple form, namely $a+b\cos^2\theta+c\cos^4\theta$, provided a single term is retained in the sum over intermediate states. It is our purpose here to prove that this result holds in fact quite generally, without any such drastic truncation of the second-order matrix element. This is already known to be true for atoms initially in s states.[3] A general formula, valid for an arbitrary hydrogenic state $|nlm\rangle$, was obtained by Zernik a few years ago.[4] Unfortunately, his analysis is somewhat obscured by an inadequate choice of the coordinate axes.

Most previous calculations of multiphoton absorption processes have explicitly assumed that the incident radiation is linearly polarized. The same assumption will be made in Sec. II, in which we give first the angular distribution for an arbitrary one-electron state in a central potential. Averaging over the magnetic quantum numbers in this formula, which looks much simpler than Zernik's, allows us to arrive at the result stated above. The correct expression of the total cross section, including an interference term previously omitted, is also given. In Sec. III we derive the corresponding formulas for circularly polarized radiation. The angular distribution for unpolarized atoms has the same simple form as in the preceding case, with, however, different coefficients a, b, c, and θ now denoting the angle between the momentum of the ejected electron and the wave vector of the incident radiation. Integration over angles yields a total cross section quite different

from that for linearly polarized radiation. The interest in this case has been stimulated by a very nice recent experiment[5] in which total three-photon ionization rates of atomic cesium by ruby-laser light have been measured for both linear and circular polarization. Finally, in Sec. IV we present more analytical and numerical results for the particular case of hydrogen. A few summation formulas for spherical harmonics used in averaging over m are derived in the Appendix.

II. LINEARLY POLARIZED RADIATION

Throughout this paper we shall restrict ourselves, for simplicity, to the one-electron central-field model. As in the case of the ordinary (first-order) photoeffect,[2] one can show, however, that taking into account the internal structure of a many-electron atom only complicates the algebra without altering the general form of the angular distribution.

In the nonrelativistic dipole approximation the two-photon ionization differential cross section given by second-order perturbation theory reads (in atomic units)

$$\frac{I_0}{I}\frac{d\sigma}{d\Omega}=\frac{\alpha}{4\pi}\left|\sum_s \frac{\langle f|\vec{\epsilon}\cdot\vec{r}|s\rangle\langle s|\vec{\epsilon}\cdot\vec{r}|i\rangle}{E_i-E_s+\omega+i0}\right|^2 \omega k\ . \tag{2.1}$$

Here $\vec{\epsilon}$ and ω are, respectively, the polarization and energy of the incident radiation, k is the momentum of the ejected electron, E_i and E_s are the energies of the initial and intermediate atomic states, I is the radiation intensity in W/cm^2, $I_0=7.019\times10^{16}$ W/cm^2, and α is the fine-structure constant. The summation runs over the whole (discrete and continuous) spectrum of the unperturbed atomic Hamiltonian, and energy conservation gives $\frac{1}{2}k^2=E_i+2\omega$.

In order to separate radial and angular variables, we introduce spherical coordinates with the polar z axis along the unit polarization vector $\vec{\epsilon}$ (Fig. 1). The dipole interaction then takes the simple form $\vec{\epsilon}\cdot\vec{r}=(4\pi/3)^{1/2}rY_{1,0}(\hat{r})$. We assume that the electron is initially in an arbitrary bound state $|i\rangle=R_{nl}(r)Y_{lm}(\hat{r})$, and use as intermediate states in Eq. (2.1) the complete set $|s\rangle=R_{\nu\lambda}(r)Y_{\lambda\mu}(\hat{r})$. The final state, which must represent asymptotically a unit amplitude plane wave with momentum $\vec{k}$ plus incoming spherical waves,[6] may be written as

$$|f\rangle=\left(\frac{\pi}{2k}\right)^{1/2}\sum_L i^L(2L+1)e^{-i\delta_L}R_{k,L}(r)P_L(\hat{k}\cdot\hat{r}). \tag{2.2}$$

For a neutral atom the radial wave functions $R_{k,L}$, normalized on the energy scale, have the asymptotic form

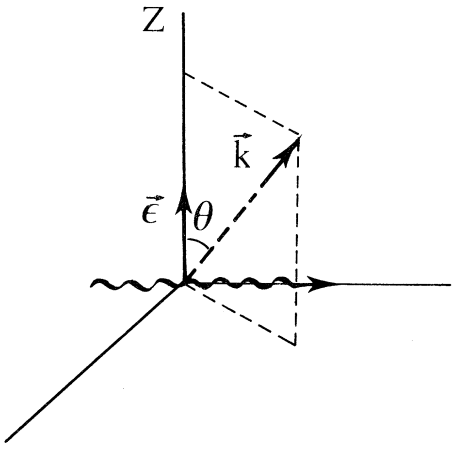

FIG. 1. Coordinate system used for linearly polarized incident radiation (θ is the angle between the direction of the ejected electron and the light polarization).

$$R_{k,L}(r)\sim(2/\pi k)^{1/2}r^{-1}\sin(kr-\pi L/2+\delta_L+k^{-1}\ln 2kr)\ . \tag{2.3}$$

In the case of a negative ion (photodetachment) the logarithmic phase is missing, because the electron moves in a potential which falls off rapidly as $r\to\infty$.

The integration over angles in the second-order matrix element is easily carried out after using the addition theorem for spherical harmonics,

$$\frac{2L+1}{4\pi}P_L(\hat{k}\cdot\hat{r})=\sum_M Y^*_{LM}(\hat{k})\,Y_{LM}(\hat{r}), \tag{2.4}$$

and yields

$$\sum_s=\left(\frac{8\pi^3}{k}\right)^{1/2}\sum_{\lambda L}(-i)^L e^{i\delta_L}(2\lambda+1)[(2L+1)(2l+1)]^{1/2}\times\begin{pmatrix}L&1&\lambda\\0&0&0\end{pmatrix}\begin{pmatrix}\lambda&1&l\\0&0&0\end{pmatrix}\begin{pmatrix}L&1&\lambda\\-m&0&m\end{pmatrix}\times\begin{pmatrix}\lambda&1&l\\-m&0&m\end{pmatrix}T_{\lambda L}(\omega)Y_{Lm}(\hat{k}), \tag{2.5}$$

where

$$T_{\lambda L}(\omega)=\sum_\nu\frac{\langle R_{k,L}|r|R_{\nu\lambda}\rangle\langle R_{\nu\lambda}|r|R_{nl}\rangle}{E_{nl}-E_{\nu\lambda}+\omega+i0}\ . \tag{2.6}$$

The sum in the right-hand side of Eq. (2.5) consists in fact of four terms, corresponding to the four distinct channels allowed by the selection rules. For further reference we shall number these channels as, say, $1(l\to l+1\to l+2)$, $2(l\to l+1\to l)$, $3(l\to l-1\to l)$, $4(l\to l-1\to l-2)$.

Substituting the explicit expressions of the 3-j symbols[7] one finds

$$\frac{I_0}{I}\left(\frac{d\sigma}{d\Omega}\right)_{nlm}=2\pi^2\alpha\omega|M_{l+2}+M_l+M_{l-2}|^2, \tag{2.7}$$

with

$$M_{l+2}=\left(\frac{(l-m+1)(l-m+2)(l+m+1)(l+m+2)}{(2l+1)(2l+3)^2(2l+5)}\right)^{1/2} T_{l+1,l+2}e^{i\delta_{l+2}}Y_{l+2,m}(\hat{k}) , \tag{2.8}$$

$$M_{l-2}=\left(\frac{(l-m)(l-m-1)(l+m)(l+m-1)}{(2l-3)(2l-1)^2(2l+1)}\right)^{1/2} T_{l-1,l-2}e^{i\delta_{l-2}}Y_{l-2,m}(\hat{k}) , \tag{2.9}$$

$$M_l=-\left(\frac{(l-m+1)(l+m+1)}{(2l+1)(2l+3)}T_{l+1,l}+\frac{(l-m)(l+m)}{(2l-1)(2l+1)}T_{l-1,l}\right)e^{i\delta_l}Y_{l,m}(\hat{k}) . \tag{2.10}$$

Equations (2.7)–(2.10) are much simpler than the corresponding Eqs. (10)–(13) in Ref. 4 owing to the choice of $\vec{\epsilon}$ as polar axis, which allowed us to take full advantage of the selection rule $\Delta m=0$ in addition to $\Delta l=\pm 1$.

The total cross section for two-quantum photoionization of a state (n, l), assuming equally populated magnetic sublevels, is readily obtained by integrating Eq. (2.7) over the angles θ, φ, which define the direction $\hat{k}$ of the ejected electron, and averaging over m. Taking into account the orthonormality relations for the spherical harmonics one gets

$$\frac{I_0}{I}\sigma_{nl}=\frac{2\pi^2\alpha}{15}\omega\left(\frac{2(l+1)(l+2)}{(2l+1)(2l+3)}|T_{l+1,l+2}|^2+\frac{2l(l-1)}{(2l-1)(2l+1)}|T_{l-1,l-2}|^2\right.$$
$$\left.+\frac{(l+1)(4l^2+8l+5)}{(2l+1)^2(2l+3)}|T_{l+1,l}|^2+\frac{l(4l^2+1)}{(2l-1)(2l+1)^2}|T_{l-1,l}|^2+\frac{4l(l+1)}{(2l+1)^2}\mathrm{Re}(T^*_{l+1,l}T_{l-1,l})\right) . \tag{2.11}$$

For $l\neq 0$ channels 2 and 3, which lead to the same final state, are both open. The last term in Eq. (2.11) arises from the interference between these two channels and has been previously omitted.[8,9]

From Eq. (2.7) it is clear that the angular distribution of electrons emitted from a state (n, l, m) does not depend on the angle φ, a consequence of the symmetry with respect to rotations about the polar axis. We shall prove now that, although the θ dependence for the different magnetic sublevels is quite intricate indeed, containing powers of $\cos\theta$ as high as $2l+4$, the observed angular distribution will assume, for an unpolarized target, the simple form mentioned in Sec. I, whatever the orbital quantum number l. To this end we use the well-known summation formulas

$$4\pi(2l+1)^{-1}\sum_m |Y_{lm}|^2=1 , \tag{2.12}$$

$$8\pi(2l+1)^{-1}\sum_m m^2|Y_{lm}|^2=l(l+1)\sin^2\theta , \tag{2.13}$$

$$8\pi(2l+1)^{-1}\sum_m m^4|Y_{lm}|^2=l(l+1)\sin^2\theta$$
$$\times[1+\tfrac{3}{4}(l-1)(l+2)\sin^2\theta] , \tag{2.14}$$

together with the identities (A2), (A3), and (A5), derived in the Appendix. Introducing for brevity the new quantities

$$X_{pp'}=\mathrm{Re}(T^*_{\lambda,L}T_{\lambda',L'}e^{i(\delta_{L'}-\delta_L)}) , \tag{2.15}$$

where the subscripts p, p', correspond, respectively, to the channels $(l\to\lambda\to L)$, $(l\to\lambda'\to L')$ one eventually gets

$$\frac{I_0}{I}\left(\frac{d\sigma}{d\Omega}\right)_{nl}=a+b\cos^2\theta+c\cos^4\theta , \tag{2.16}$$

where

$$a=\frac{\pi\alpha}{16}\omega(2l+1)^{-2}\left(\frac{(l+1)(l+2)(3l^2+5l+4)}{(2l+3)^2}(X_{11}+X_{22}+2X_{12})+\frac{l(l-1)(3l^2+l+2)}{(2l-1)^2}(X_{33}+X_{44}+2X_{34})\right.$$
$$\left.+\frac{6(l-1)l(l+1)(l+2)}{(2l-1)(2l+3)}(X_{13}+X_{14}+X_{23}+X_{24})\right) , \tag{2.17}$$

$$b=\frac{\pi\alpha}{8}\omega(2l+1)^{-2}\left(\frac{l+1}{(2l+3)^2}[(l+2)(l+3)(l-4)X_{11}+l(l^2+5l+8)X_{22}-6(l+2)(l^2+l+2)X_{12}]\right.$$
$$+\frac{l}{(2l-1)^2}[(l+1)(l^2-3l+4)X_{33}+(l-1)(l-2)(l+5)X_{44}-6(l-1)(l^2+l+2)X_{34}]$$
$$\left.+\frac{2l(l+1)}{(2l-1)(2l+3)}[(l^2+l+6)X_{23}-3(l-1)(l+4)X_{24}-3(l+2)(l-3)X_{13}-15(l-1)(l+2)X_{14}]\right) , \tag{2.18}$$

$$c=\frac{\pi\alpha}{16}\,\omega(2l+1)^{-2}\left(\frac{(l+1)(l+2)}{(2l+3)^2}\,[3(l+3)(l+4)X_{11}+3l(l-1)X_{22}-10l(l+3)X_{12}]\right.$$
$$+\frac{l(l-1)}{(2l-1)^2}\,[3(l+1)(l+2)X_{33}+3(l-2)(l-3)X_{44}-10(l+1)(l-2)X_{34}]$$
$$\left.+\frac{2l(l+1)}{(2l-1)(2l+3)}\,[3(l-1)(l+2)X_{23}-5(l-1)(l-2)X_{24}-5(l+2)(l+3)X_{13}+35(l-1)(l+2)X_{14}]\right)\ . \qquad (2.19)$$

Alternatively, one can express the averaged differential cross section of Eq. (2.16) in terms of Legendre polynomials:

$$\frac{I_0}{I}\left(\frac{d\sigma}{d\Omega}\right)_{nl}=A+BP_2(\cos\theta)+CP_4(\cos\theta)\ , \qquad (2.20)$$

where, in particular, $A=(1/4\pi)(I_0/I)\sigma_{nl}$.

III. CIRCULARLY POLARIZED RADIATION

Fox, Kogan, and Robinson[5] recently reported preliminary experimental evidence for the ionization of atomic cesium by simultaneous absorption of three ruby-laser quanta, and indicated that the efficiency of the process depended on the state of polarization of the incident radiation, even though the atoms were unpolarized. They also offered a physical explanation of this interesting effect, which does not occur in ordinary photoionization, by noticing that polarized radiation generates polarized intermediate atomic states. This induced polarization will manifest itself in the subsequent virtual transitions and finally in the total rate of the process.

To get further insight into this polarization effect, it seemed helpful to investigate the situation in the somewhat simpler case of two-photon ionization.[10] Specifically, we shall start anew the calculation of Sec. II by assuming that the incident radiation is (right-hand) circularly polarized, instead of being linearly polarized. In this case it will be more convenient to choose the polar z axis along the photon wave vector (Fig. 2). The dipole interaction operator then reduces to $\vec{\epsilon}\cdot\vec{r}=-(4\pi/3)^{1/2}rY_{1,1}(\hat{r})$, and the integration over angles in the second-order matrix element of Eq. (2.1) yields

$$\sum_s=-\left(\frac{8\pi^3}{k}\right)^{1/2}\sum_{\lambda L}(-i)^L e^{i\delta_L}(2\lambda+1)[(2L+1)(2l+1)]^{1/2}$$
$$\times\begin{pmatrix}L&1&\lambda\\0&0&0\end{pmatrix}\begin{pmatrix}\lambda&1&l\\0&0&0\end{pmatrix}\begin{pmatrix}L&1&\lambda\\-m-2&1&m+1\end{pmatrix}\begin{pmatrix}\lambda&1&l\\-m-1&1&m\end{pmatrix}T_{\lambda L}(\omega)Y_{L,m+2}(\hat{k})\ , \qquad (3.1)$$

where $T_{\lambda L}$ are the reduced transition amplitudes defined in Eq. (2.6). Instead of Eq. (2.7) one finds now

$$\frac{I_0}{I}\left(\frac{d\sigma'}{d\Omega}\right)_{nlm}=\frac{\pi^2\alpha}{2}\,\omega\,|M'_{l+2}+M'_l+M'_{l-2}|^2\ , \qquad (3.2)$$

with

$$M'_{l+2}=\left(\frac{(l+m+1)(l+m+2)(l+m+3)(l+m+4)}{(2l+1)(2l+3)^2(2l+5)}\right)^{1/2}T_{l+1,l+2}e^{i\delta_{l+2}}Y_{l+2,m+2}(\hat{k})\ , \qquad (3.3)$$

$$M'_{l-2}=\left(\frac{(l-m)(l-m-1)(l-m-2)(l-m-3)}{(2l-3)(2l-1)^2(2l+1)}\right)^{1/2}T_{l-1,l-2}e^{i\delta_{l-2}}Y_{l-2,m+2}(\hat{k})\ , \qquad (3.4)$$

$$M'_l=\left(\frac{(l-m)(l-m-1)(l+m+1)(l+m+2)}{(2l+1)^2}\right)^{1/2}\left(\frac{1}{2l+3}\,T_{l+1,l}+\frac{1}{2l-1}\,T_{l-1,l}\right)e^{i\delta_l}Y_{l,m+2}(\hat{k})\ . \qquad (3.5)$$

Integrating over $\hat{k}$ and averaging over m, one further gets for the total cross section the result

$$\frac{I_0}{I}\,\sigma'_{nl}=\frac{2\pi^2\alpha}{15}\,\omega\left(\frac{3(l+1)(l+2)}{(2l+1)(2l+3)}\,|T_{l+1,l+2}|^2+\frac{3l(l-1)}{(2l-1)(2l+1)}\,|T_{l-1,l-2}|^2\right.$$
$$\left.+\frac{l(l+1)(2l-1)}{2(2l+1)^2(2l+3)}\,|T_{l+1,l}|^2+\frac{l(l+1)(2l+3)}{2(2l-1)(2l+1)^2}\,|T_{l-1,l}|^2+\frac{l(l+1)}{(2l+1)^2}\,\mathrm{Re}(T^*_{l+1,l}T_{l-1,l})\right), \qquad (3.6)$$

which is clearly different from the corresponding expression in Eq. (2.11).

Using again Eqs. (2.12)–(2.14), and the new summation formulas (A7), (A9), and (A11), given in the Appendix, it is readily shown that the angular distribution of the photoelectrons emitted from an unpolarized state (n, l) has a general form similar to Eq. (2.16). We prefer, however, to express the result in this

case in the equivalent form

$$\frac{I_0}{I}\left(\frac{d\sigma'}{d\Omega}\right)_{nl} = a' + b' \sin^2\theta + c' \sin^4\theta \ . \tag{3.7}$$

The coefficients are found to be

$$a' = \frac{\pi\alpha}{8}\,\omega(2l+1)^{-2}(l-1)\,l(l+1)\,(l+2)\left(\frac{1}{(2l+3)^2}\,(X_{11}+X_{22}+2X_{13}) + \frac{1}{(2l-1)^2}\,(X_{33}+X_{44}+2X_{34}) + \frac{2}{(2l-1)\,(2l+3)}\,(X_{13}+X_{14}+X_{23}+X_{24})\right) , \tag{3.8}$$

$$b' = \frac{\pi\alpha}{8}\,\omega(2l+1)^{-2}\,l(l+1)\left(\frac{1}{(2l+3)^2}\,[3(l+2)\,(l+3)X_{11} - (l^2+l-3)X_{22} - 2(l-3)\,(l+2)X_{12}] + \frac{1}{(2l-1)^2}\,[3(l-1)\,(l-2)X_{44} - (l^2+l-3)X_{33} - 2(l-1)\,(l+4)X_{34}] - \frac{2}{(2l-1)\,(2l+3)} \times [(l-3)\,(l+2)X_{13} + 5(l-1)\,(l+2)X_{14} + (l^2+l-3)X_{23} + (l-1)\,(l+4)X_{24}]\right) , \tag{3.9}$$

$$c' = \frac{\pi\alpha}{64}\,\omega(2l+1)^{-2}\left(\frac{1}{(2l+3)^2}\,[3(l+1)_4X_{11} + 3(l-1)_4X_{22} - 10(l)_4X_{12}] + \frac{1}{(2l-1)^2}\,[3(l-1)_4X_{33} + 3(l-3)_4X_{44} - 10(l-2)_4X_{34}] + \frac{2}{(2l-1)\,(2l+3)}\,[3(l-1)_4X_{23} + 35(l-1)_4X_{14} - 5(l)_4X_{13} - 5(l-2)_4X_{24}]\right) , \tag{3.10}$$

where we have used for simplicity the notation $(\lambda)_4 = \lambda(\lambda+1)(\lambda+2)(\lambda+3)$. The ten quantities X_{ij}, are, of course, those already defined in Sec. II.

In terms of Legendre polynomials one has

$$\frac{I_0}{I}\left(\frac{d\sigma'}{d\Omega}\right)_{nl} = A' + B'P_2(\cos\theta) + C'P_4(\cos\theta) \ , \tag{3.11}$$

where $A' = (1/4\pi)(I_0/I)\sigma'_{nl}$.

Important simplifications occur in the particular case of s states. Equation (2.11), for instance, reduces to

$$\frac{I_0}{I}\,\sigma = \frac{2\pi^2\alpha}{45}\,\omega(4X_{11} + 5X_{22}) \ , \tag{3.12}$$

while in Eq. (3.6) only a single term subsists:

$$\frac{I_0}{I}\,\sigma' = \frac{4\pi^2\alpha}{15}\,\omega X_{11} \ , \tag{3.13}$$

since for right-hand (left-hand) circularly polarized radiation channel 2 is forbidden by the selection rule $\Delta m = +1$ ($\Delta m = -1$). Hence, the ratio of the total two-photon ionization rates for circular versus linear polarization is

$$\sigma'/\sigma = 6(4 + 5X_{22}/X_{11})^{-1} \ . \tag{3.14}$$

According to their definition, both X_{11} and X_{22} are non-negative, and therefore the maximum value of the above ratio is $\frac{3}{2}$. This happens to be quite close to the experimental value of 1.28 ± 0.2 reported in the case of cesium.[10]

More generally, it may be shown[11] that the theoretically allowed maximum value of the ratio σ'/σ for N-photon ionization is $(2N-1)!!/N!$. For $N=3$ this gives $\frac{5}{2}$, which is also just above the experimental result[5] of 2.15 ± 0.4 for cesium irradiated with ruby-laser light.[12]

The differential cross sections also become simpler for $l=0$. In particular, as seen from Eqs. (3.8) and (3.9), in this case one has $a' = b' = 0$, so that the angular distribution must be proportional to $\sin^4\theta$.[13]

For arbitrary l, Eqs. (2.11) and (3.6) can be combined to give

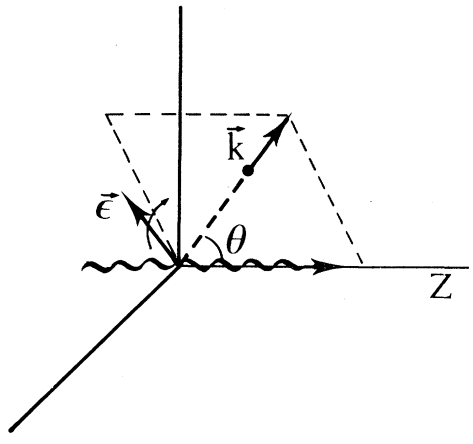

FIG. 2. Coordinate system used for circularly polarized incident radiation (θ is the angle between the direction of the ejected electron and that in which the light propagates).

TABLE I. Total cross sections per unit intensity for the two-photon ionization of hydrogen in the $1s$ state by linearly (σ) and circularly (σ') polarized radiation, in cm^4/W. Numbers in parentheses indicate powers of 10.

λ (Å)	σ/I	σ'/I	σ'/σ
982	•••	•••	1.500
1003	1.808(−34)	•••	3.278(−1)
1007	•••	8.626(−37)	4.036(−3)
1025.83	∞	∞	1.216
1054	•••	•••	1.500
1122	3.034(−34)	•••	3.153(−1)
1136	•••	2.381(−38)	6.371(−5)
1215.68	∞	∞	1.295
1420	•••	•••	1.500
1823.52	1.170(−32)	1.666(−32)	1.425

$$\tfrac{3}{2}\sigma - \sigma' = \gamma \left| \frac{l+1}{2l+1}\, T_{l+1,l} + \frac{l}{2l+1}\, T_{l-1,l} \right|^2 , \quad (3.15)$$

where $\gamma = (I/I_0)(\pi^2\alpha/3)\omega$. This clearly shows that the maximum value of the ratio σ'/σ is equal to $\frac{3}{2}$, exactly as found above for s states.

IV. TWO-PHOTON IONIZATION RATES IN HYDROGEN

The one-electron model provides an adequate approximation for a large number of atomic systems, including alkali atoms,[14] negative ions,[15] and so on. However, in all these cases, for the calculation of the transition amplitudes $T_{\lambda L}$ it is necessary to resort to numerical methods, either for summing term by term over the intermediate states or for integrating an inhomogeneous radial equation.

In the particular case of a pure Coulomb potential, i.e., for hydrogenic atoms, the relevant second-order matrix elements can be evaluated analytically in closed form.[3,16] This is achieved by rewriting Eq. (2.6) as

$$T_{\lambda L}(\omega) = \langle R_{k,L} | r G_\lambda(W) r | R_{nl} \rangle , \quad W = E_n + \omega + i0 \quad (4.1)$$

TABLE II. Total cross sections per unit intensity for the two-photon ionization of hydrogen in the $2s$ state by linearly (σ) and circularly (σ') polarized radiation, in cm^4/W. Numbers in parentheses indicate powers of 10.

λ (Å)	σ/I	σ'/I	σ'/σ
4479	•••	•••	1.500
4603	5.578(−32)	•••	2.677(−1)
4628	•••	8.391(−37)	1.233(−5)
4861.33	∞	∞	1.261
5243	•••	•••	1.500
5596	1.263(−31)	•••	2.794(−1)
5667	•••	3.661(−38)	2.373(−7)
6562.79	∞	∞	1.312
7294.08	2.427(−29)	3.464(−29)	1.427

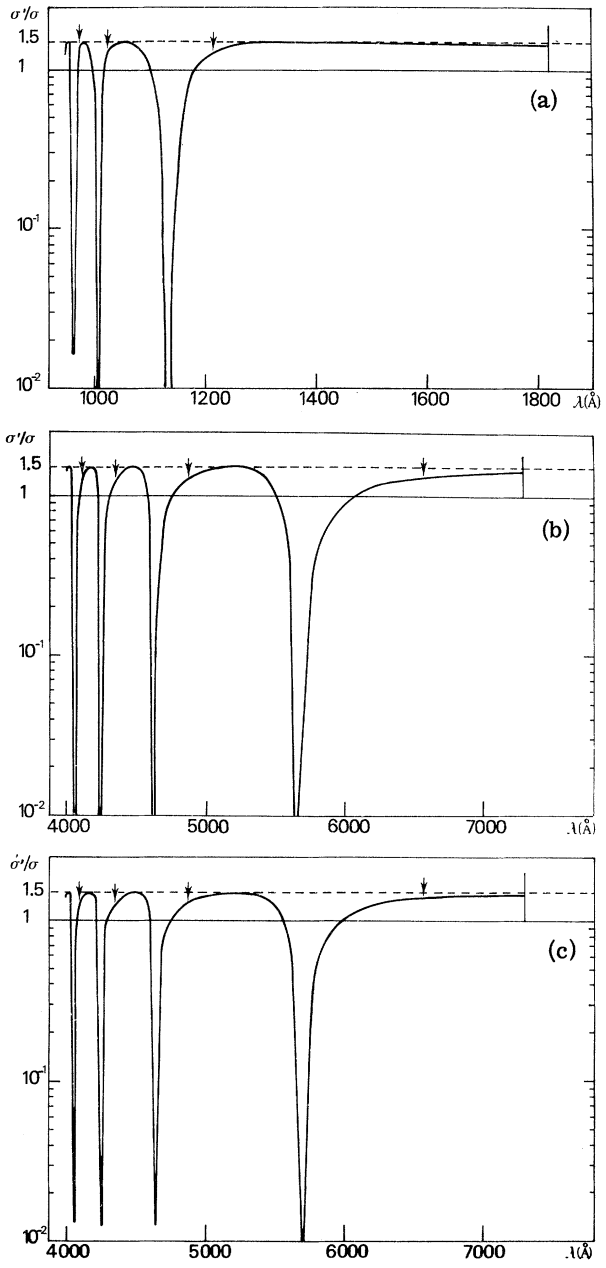

FIG. 3. Ratio σ'/σ for two-photon ionization from the hydrogenic states (a) $1s$, (b) $2s$, and (c) $2p$. Arrows indicate the positions of resonances.

where

$$G_\lambda(W) = \sum_\nu \frac{|R_{\nu\lambda}\rangle \langle R_{\nu\lambda}|}{W - E_\nu} \quad (4.2)$$

is the radial Coulomb Green's function for angular momentum λ, which is known explicitly. The discrete energy levels are in this case $E_n = -1/2n^2$ (l degeneracy), and the phase shifts in Eq. (2.3) are given by $\delta_L = \eta_L \equiv \arg\Gamma(L+1-i\eta)$, $\eta = 1/k$.

Substituting in Eq. (4.1) the wave functions for

TABLE III. Total cross sections per unit intensity for the two-photon ionization of hydrogen in the $2p$ state by linearly (σ) and circularly (σ') polarized radiation, in cm^4/W. Numbers in parentheses indicate powers of 10.

λ (Å)	σ/I	σ'/I	σ'/σ
4480	•••	•••	1.500
4620	2.274(−32)	•••	2.226(−1)
4638	•••	3.231(−34)	1.232(−2)
4861.33	∞	∞	1.328
5260	•••	•••	1.500
5650	6.435(−32)	•••	2.012(−1)
5696	•••	7.792(−34)	1.065(−2)
6562.79	∞	∞	1.398
7294.08	2.922(−29)	4.289(−29)	1.468

the initial nl state and for the final state, together with an integral representation of G_λ, one finds

$$T_{\lambda L}(\omega) = -2C'_{k,L}C_{nl}\int_0^\infty dt\,(\coth\tfrac{1}{2}t)^{2\alpha} \times\int_0^\infty dr'\,r'^{3/2}e^{-(\cosh t/\xi)r'}M_{i\eta,L+1/2}(-2ikr') \times\int_0^\infty dr\,r^{3/2}e^{-(\cosh t/\xi)r}M_{n,l+1/2}(2r/n) \times I_{2\lambda+1}[2(rr')^{1/2}\sinh t/\xi]\,, \quad (4.3)$$

where

$$C_{nl} = \frac{1}{n(2l+1)!}\left(\frac{(n+l)!}{(n-l-1)!}\right)^{1/2} \quad (4.4)$$

and

$$C'_{k,L} = i^{L+1}(2\pi k)^{-1/2}e^{\pi\eta/2}\left|\Gamma(L+1-i\eta)\right|/(2L+1)! \quad (4.5)$$

are normalization constants, and $M_{\lambda,\mu}(z)$ denotes the regular Whittaker confluent hypergeometric function.

The parameters ξ and η are related to the photon energy ω (in a.u.) by

$$\xi = n(1-2n^2\omega)^{-1/2}\,, \quad \eta = n(4n^2\omega-1)^{-1/2}\,, \quad (4.6)$$

and are both real in the interval between the thresholds for two-photon and one-photon ionization.

From the calculation it becomes apparent that any of the required amplitudes $T_{\lambda L}$ may be expressed as a combination of at most three Appell hypergeometric functions of two variables of type F_1, one of which is degenerated. It seems, however, difficult to state this result in a single general formula covering the four possible channels.

Hereafter we present the explicit expressions obtained for the different transition amplitudes appropriate for the two-photon ionization of the lowest-lying states, with principal quantum numbers $n=1$ and $n=2$.

For s states only two amplitudes are involved, namely, $T_{1,2}$ and $T_{1,0}$, corresponding, respectively, to channels 1 and 2. Their expressions are as follows:

1*s state*:

$$T_{1,2} = \left(\frac{2}{\pi}\right)^{1/2}2^9\xi^{10}\eta^{11/2}e^{-\eta\varphi}e^{\pi\eta/2}\left|\Gamma(3-i\eta)\right|(1-\xi)^{-1}(2-\xi)^{-1}(1+\xi)^{-5}(\xi^2+\eta^2)^{-4} \times\left[F_1(2-\xi;3+i\eta,3-i\eta;3-\xi;z,z') - \frac{2-\xi}{4-\xi}\left(\frac{1-\xi}{1+\xi}\right)^2F_1(4-\xi;3+i\eta,3-i\eta;5-\xi;z,z')\right], \quad (4.7)$$

$$T_{1,0} = \left(\frac{2}{\pi}\right)^{1/2}\xi^8\eta^{15/2}e^{-\eta\varphi}e^{\pi\eta/2}\left|\Gamma(1-i\eta)\right|(2-\xi)^{-1}(1+\xi)^{-5}(\xi^2+\eta^2)^{-4}\left[(1-2\xi)F_1(2-\xi;3+i\eta,3-i\eta;3-\xi;z,z') - (1+2\xi)\frac{2-\xi}{4-\xi}\left(\frac{1-\xi}{1+\xi}\right)F_1(4-\xi;3+i\eta,3-i\eta;5-\xi;z,z') + 12(2-\xi)(1+\xi)^{-1}(1-z)^{-3-i\eta}(1-z')^{-3+i}\right], \quad (4.8)$$

where

$$\xi = (1-x)^{-1/2}\,, \quad \eta = (2x-1)^{-1/2}\,, \quad \varphi = 2\arctan(\xi/\eta)\,, \quad x = 2\omega\ \text{(a.u.)}\,,$$

and

$$z = \frac{1-\xi}{1+\xi}\left(\frac{\eta+i\xi}{\eta-i\xi}\right)\,, \quad z' = \frac{1-\xi}{1+\xi}\left(\frac{\eta-i\xi}{\eta+i\xi}\right)\,. \quad (4.9)$$

2*s state*:

$$T_{1,2} = \pi^{-1/2}2^{14}\xi^{10}\eta^{11/2}e^{-\eta\varphi}e^{\pi\eta/2}\left|\Gamma(3-i\eta)\right|(2-\xi)^{-2}(2+\xi)^{-5}(\xi^2+\eta^2)^{-4}\left[F_1(2-\xi;3+i\eta,3-i\eta;3-\xi;z,z') - \frac{2-\xi}{4-\xi}\left(\frac{2-\xi}{2+\xi}\right)^2F_1(4-\xi;3+i\eta,3-i\eta;5-\xi;z,z') - 16\xi^2(2+\xi)^{-3}(1-z)^{-3-i\eta}(1-z')^{-3+i\eta}\right], \quad (4.10)$$

$$T_{1,0} = \pi^{-1/2}2^{12}\xi^8\eta^{15/2}e^{-\eta\varphi}e^{\pi\eta/2}\left|\Gamma(1-i\eta)\right|(2-\xi)^{-1}(2+\xi)^{-5}(\xi^2+\eta^2)^{-4}\left[(2-5\xi)F_1(2-\xi;3+i\eta,3-i\eta;3-\xi;z,z') - (2+5\xi)\frac{2-\xi}{4-\xi}\left(\frac{2-\xi}{2+\xi}\right)F_1(4-\xi;3+i\eta;3-i\eta;5-\xi;z,z') - 16(\xi^2-12)(2+\xi)^{-2}(1-z)^{-3-i\eta}(1-z')^{-3+i\eta}\right], \quad (4.11)$$

where

$$\xi = 2(1-x)^{-1/2}\,, \quad \eta = 2(2x-1)^{-1/2}\,, \quad \varphi = 2\arctan(\xi/\eta)\,, \quad x = 8\omega \text{ (a.u.)}\,,$$

and

$$z = \frac{2-\xi}{2+\xi}\left(\frac{\eta+i\xi}{\eta-i\xi}\right)\,, \quad z' = \frac{2-\xi}{2+\xi}\left(\frac{\eta-i\xi}{\eta+i\xi}\right)\,. \tag{4.12}$$

For p states three amplitudes are involved, namely, $T_{2,3}$, $T_{2,1}$, and $T_{0,1}$. They correspond, respectively, to channels 1, 2, and 3. One finds the following:

2p state:

$$T_{2,3} = (3\pi)^{-1/2}2^{17}\xi^{12}\eta^{13/2}e^{-\eta\varphi}e^{\pi\eta/2}\,|\,\Gamma(4-i\eta)|\,(2-\xi)^{-1}(3-\xi)^{-1}(2+\xi)^{-7}(\xi^2+\eta^2)^{-5}$$
$$\times\left[F_1(3-\xi;4+i\eta,4-i\eta;4-\xi;z,z') - \frac{3-\xi}{5-\xi}\left(\frac{2-\xi}{2+\xi}\right)^2 F_1(5-\xi;4+i\eta,4-i\eta;6-\xi;z,z')\right]\,, \tag{4.13}$$

$$T_{2,1} = (3\pi)^{-1/2}2^{14}\xi^{10}\eta^{17/2}e^{-\eta\varphi}e^{\pi\eta/2}\,|\,\Gamma(2-i\eta)|\,(3-\xi)^{-1}(2+\xi)^{-7}(\xi^2+\eta^2)^{-5}\left[(18-11\xi)F_1(3-\xi;4+i\eta,4-i\eta;4-\xi;z,z')\right.$$
$$\left. - (18+11\xi)\frac{3-\xi}{5-\xi}\left(\frac{2-\xi}{2+\xi}\right)F_1(5-\xi;4+i\eta,4-i\eta;6-\xi;z,z') + 160(3-\xi)(2+\xi)^{-1}(1-z)^{-4-i\eta}(1-z')^{-4+i\eta}\right]\,, \tag{4.14}$$

$$T_{0,1} = -(3\pi)^{-1/2}2^{11}\xi^{10}\eta^{9/2}e^{-\eta\varphi}e^{\pi\eta/2}\,|\,\Gamma(2-i\eta)|\,(1-\xi)^{-1}(2-\xi)^{-2}(2+\xi)^{-4}(\xi^2+\eta^2)^{-3}\left[F_1(1-\xi;2+i\eta,2-i\eta;2-\xi;z,z')\right.$$
$$\left. - \frac{1-\xi}{3-\xi}\left(\frac{2-\xi}{2+\xi}\right)^2 F_1(3-\xi;2+i\eta,2-i\eta;4-\xi;z,z') + 32(1-\xi)(2+\xi)^{-2}(1-z)^{-2-i\eta}(1-z')^{-2+i\eta}\right]\,, \tag{4.15}$$

where ξ, η, φ, and x are the same as for the $2s$ state.

The double series expansions of the Appell functions converge very rapidly when ω varies between the thresholds for two-photon and one-photon ionization, i.e., $\frac{1}{2} < x < 1$. In Tables I–III we have listed a few values of the total cross sections per unit intensity for linearly and circularly polarized incident radiation, computed, respectively, from Eqs. (2.11) and (3.6) in conjunction with Eqs. (4.7)–(4.15). The represented wavelengths include the two-photon threshold, resonances, relative minima of σ or σ', as well as minima and maxima of the ratio σ'/σ. The latter is seen to attain effectively the theoretically allowed value of $\frac{3}{2}$ (to within the usual roundoff). On the other hand, for the $2p$ state the ratio σ'/σ never goes so low as it does for the s states. This is probably due to the fact that for $l \neq 0$ even with circularly polarized light there is more than one channel open. A more intuitive representation of the ratio σ'/σ as a function of the incident wavelength is given in Fig. 3. It is interesting to notice that in the interval extending from the two-photon threshold up to the first resonance ionization by circularly polarized light is more efficient than by linearly polarized light. This is true also in the vicinity of the other resonances, although the ratio σ'/σ does not reach its highest values at the latter.

APPENDIX

All the summation formulas needed for the present calculation can be obtained in an elementary way by using recurrence relations among spherical harmonics in conjunction with Eqs. (2.12)–(2.14).

For instance, after multiplying

$$\cos\theta\, Y_{l+1,m} = \left(\frac{(l+2)^2-m^2}{(2l+3)(2l+5)}\right)^{1/2} Y_{l+2,m} + \left(\frac{(l+1)^2-m^2}{(2l+1)(2l+3)}\right)^{1/2} Y_{l,m} \tag{A1}$$

with its complex conjugate and with $\lambda^2 - m^2$, one easily gets

$$2\sum_m (\lambda^2-m^2)\left(\frac{(l+1)^2-m^2}{(2l+1)(2l+3)}\right)^{1/2}\left(\frac{(l+2)^2-m^2}{(2l+3)(2l+5)}\right)^{1/2} Y^*_{l+2,m}Y_{l,m}$$
$$= \frac{1}{16\pi}\,\frac{(l+1)(l+2)}{2l+3}\,\{8\lambda^2 - 4[3\lambda^2 + l(l+3)]\sin^2\theta + 5l(l+3)\sin^4\theta\}\,. \tag{A2}$$

The substitution $l \to l-2$ then gives

$$2\sum_m(\lambda^2-m^2)\left(\frac{l^2-m^2}{(2l+1)(2l-1)}\right)^{1/2}\left(\frac{(l-1)^2-m^2}{(2l-1)(2l-3)}\right)^{1/2}Y^*_{l-2,m}Y_{l,m}$$
$$=\frac{1}{16\pi}\,\frac{l(l-1)}{2l-1}\{8\lambda^2-4[3\lambda^2+(l+1)(l-2)]\sin^2\theta+5(l+1)(l-2)\sin^4\theta\}\,. \quad \text{(A3)}$$

Similarly, from the relation

$$\cos^2\theta\,Y_{l,m}=\left(\frac{(l+1)^2-m^2}{(2l+1)(2l+3)}\right)^{1/2}\left(\frac{(l+2)^2-m^2}{(2l+3)(2l+5)}\right)^{1/2}Y_{l+2,m}$$
$$+\frac{2l(l+1)-2m^2-1}{(2l-1)(2l+3)}\,Y_{l,m}+\left(\frac{l^2-m^2}{(2l+1)(2l-1)}\right)^{1/2}\left(\frac{(l-1)^2-m^2}{(2l-1)(2l-3)}\right)^{1/2}Y_{l-2,m} \quad \text{(A4)}$$

one obtains

$$2\sum_m\left(\frac{(l-1)^2-m^2}{(2l-3)(2l-1)}\right)^{1/2}\left(\frac{l^2-m^2}{(2l-1)(2l+1)}\right)\left(\frac{(l+1)^2-m^2}{(2l+1)(2l+3)}\right)^{1/2}\left(\frac{(l+2)^2-m^2}{(2l+3)(2l+5)}\right)^{1/2}Y^*_{l+2,m}Y_{l-2,m}$$
$$=\frac{1}{16\pi}\,\frac{(l-1)\,l(l+1)(l+2)}{(2l-1)(2l+1)(2l+3)}\,(8-40\sin^2\theta+35\sin^4\theta)=\frac{1}{2\pi}\,\frac{(l-1)\,l(l+1)(l+2)}{(2l-1)(2l+1)(2l+3)}\,P_4(\cos\theta)\,. \quad \text{(A5)}$$

On the other hand, the relation

$$\sin\theta\,e^{i\varphi}Y_{l+1,m+1}=\left(\frac{(l+m+3)(l+m+4)}{(2l+3)(2l+5)}\right)^{1/2}Y_{l+2,m+2}-\left(\frac{(l-m)(l-m-1)}{(2l+1)(2l+3)}\right)^{1/2}Y_{l,m+2} \quad \text{(A6)}$$

leads to

$$2\sum_m(l+m+1)(l+m+2)\left(\frac{(l-m)(l-m-1)(l+m+3)(l+m+4)}{(2l+1)(2l+3)^2(2l+5)}\right)^{1/2}Y^*_{l+2,m+2}Y_{l,m+2}$$
$$=\frac{1}{16\pi}\,\frac{l(l+1)(l+2)}{2l+3}\,[8(l-1)-8(l-3)\sin^2\theta-5(l+3)\sin^4\theta]\,, \quad \text{(A7)}$$

and the relation

$$\sin\theta\,e^{i\varphi}Y_{l-1,m+1}=\left(\frac{(l+m+1)(l+m+2)}{(2l-1)(2l+1)}\right)^{1/2}Y_{l,m+2}-\left(\frac{(l-m-2)(l-m-3)}{(2l-1)(2l-3)}\right)^{1/2}Y_{l-2,m+2}\,, \quad \text{(A8)}$$

which is simply obtained from (A6) by changing l in $l-2$, yields

$$2\sum_m(l-m)(l-m-1)\left(\frac{(l-m-2)(l-m-3)(l+m+1)(l+m+2)}{(2l-3)(2l-1)^2(2l+1)}\right)^{1/2}Y^*_{l-2,m+2}Y_{l,m+2}$$
$$=\frac{1}{16\pi}\,\frac{l(l-1)(l+1)}{2l-1}\,[8(l+2)-8(l+4)\sin^2\theta-5(l-2)\sin^4\theta]\,. \quad \text{(A9)}$$

Finally, from

$$\sin^2\theta\,e^{2i\varphi}Y_{l,m}=\left(\frac{(l+m+1)(l+m+2)(l+m+3)(l+m+4)}{(2l+1)(2l+3)^2(2l+5)}\right)^{1/2}Y_{l+2,m+2}$$
$$-2\left(\frac{(l-m)(l-m-1)(l+m+1)(l+m+2)}{(2l-1)^2(2l+3)^2}\right)^{1/2}Y_{l,m+2}+\left(\frac{(l-m)(l-m-1)(l-m-2)(l-m-3)}{(2l-3)(2l-1)^2(2l+1)}\right)^{1/2}Y_{l-2,m+2} \quad \text{(A10)}$$

it follows that

$$2\sum_m\left(\frac{(l-m)\cdots(l-m-3)(l+m+1)\cdots(l+m+4)}{(2l-3)(2l+5)}\right)^{1/2}Y^*_{l+2,m+2}Y_{l-2,m+2}$$
$$=\frac{1}{16\pi}\,(l-1)\,l(l+1)(l+2)[8-40\sin^2\theta+35\sin^4\theta]=\frac{1}{2\pi}\,(l-1)\,l(l+1)(l+2)P_4(\cos\theta)\,. \quad \text{(A11)}$$

---

*Laboratoire Associé au Centre National de la Recherche Scientifique.

[1]H. A. Bethe and E. E. Salpeter, *Quantum Mechanics of One- and Two-Electron Atoms* (Academic, New York, 1957), Sec. 72.

[2]J. Cooper and R. N. Zare, in *Lectures in Theoretical Physics*, edited by S. Geltman, K. T. Mahanthappa, and W. E. Brittin (Gordon and Breach, New York, 1969), Vol. XI-C.

[3]S. Klarsfeld, Nuovo Cimento Lett. **2**, 548 (1969); Nuovo Cimento Lett. **3**, 395 (1970). As a matter of fact, such results appear to be special cases of the so-called rules restricting the complexity of angular distributions in reactions which involve photons. See, for instance, C. N. Yang, Phys. Rev. **74**, 764 (1948); and M. Morita, A. Sugie, and S. Yoshido, Prog. Theor. Phys. **12**, 713 (1954).

[4]W. Zernik, Phys. Rev. **135**, A51 (1964).

[5]R. A. Fox, R. M. Kogan, and E. J. Robinson, Phys. Rev. Lett. **26**, 1416 (1971).

[6]G. Breit and H. A. Bethe, Phys. Rev. **93**, 888 (1954).

[7]See A. R. Edmonds, *Angular Momentum in Quantum Mechanics* (Princeton U.P., Princeton, N. J., 1957); or D. M. Brink and G. R. Satchler, *Angular Momentum* (Oxford U. P., London, 1962).

[8]W. Zernik and R. W. Klopfenstein, J. Math. Phys. **6**, 262 (1965).

[9]W. Zernik, Phys. Rev. **176**, 420 (1968).

[10]In a subsequent experiment R. M. Kogan, R. A. Fox, G. T. Burnham, and E. J. Robinson [Bull. Am. Phys. Soc. **16**, 1411 (1971)] also observed the two-photon ionization of atomic cesium by the second harmonic of the ruby laser.

[11]S. Klarsfeld and A. Maquet, Phys. Rev. Lett. **29**, 79 (1972).

[12]For $N=2$, $N=3$, and an initial s state, the angular distribution and the maximum allowed ratio σ'/σ have been obtained in a somewhat different way by P. Lambropoulos [Phys. Rev. Lett. **28**, 585 (1972)].

[13]Cross sections for N-photon ionization of s states with circularly polarized light have been discussed very recently by P. Lambropoulos [Phys. Rev. Lett. **29**, 453 (1972)].

[14]H. B. Bebb, Phys. Rev. **149**, 25 (1966); Phys. Rev. **153**, 23 (1967).

[15]E. J. Robinson and S. Geltman, Phys. Rev. **153**, 4 (1967).

[16]L. P. Rapoport, B. A. Zon, and L. P. Manakov, Zh. Eksp. Teor. Fiz. **55**, 924 (1968) [Sov. Phys.-JETP **28**, 480 (1969)]; Zh. Eksp. Teor. Fiz. **56**, 400 (1969) [Sov. Phys.-JETP **29**, 220 (1969)].

PHYSICAL REVIEW A VOLUME 7, NUMBER 5 MAY 1973

Compton Scattering of High-Energy Electrons from Helium*†

H. F. Wellenstein and R. A. Bonham

Department of Chemistry, Indiana University, Bloomington, Indiana 47401

(Received 19 June 1972; revised manuscript received 5 September 1972)

The electron-impact energy-loss spectrum of He at a scattering angle of 7° has been measured with an energy resolution of 2.7 eV full width at half-maximum using 25-keV incident electrons. A binary-encounter approximation was used to obtain the electron Compton profile from the cross-section differential with respect to both the energy loss of the incident electron and solid angle of the scattered electron $d^2\sigma/dEd\Omega$. The electron Compton profile was corrected for interference scattering from pairs of target electrons and exchange. It was then compared to theoretical and x-ray experimental values for the Compton profile. The effects of background, multiple scattering, and energy resolution are discussed. The electron-impact and x-ray methods for measuring Compton profiles are compared.

I. INTRODUCTION

In 1923 Compton[1] reported that the spectral line of the inelastically scattered x rays was significantly broadened, and Du Mond[2] in 1929 derived a Doppler-broadening theory which pointed out that Compton scattering should be ideal for the measurements of momentum distributions of the electrons in molecules. But it has only been recently[3–8] that such experiments were performed with a high enough accuracy to make meaningful comparisons between theory and experiment. An excellent review of the literature up to 1971 has been given by Cooper.[9] All recent studies have been performed using x rays, although as Hughes and Mann[10] showed in 1938 the energy spectrum obtained from electron scattering shows the same characteristic Compton profile. They did not, however, obtain good agreement with the theory[11,12] which Duncanson[13] ascribed to multiple scattering. This discouraged all further work using electron sources, which was unfortunate, and the authors will attempt to show, using He as an example, that high-energy-electron spectroscopy is in most aspects superior to photon scattering.

II. EXPERIMENT

The high-energy-electron spectrometer used in these studies has been partially described in an earlier paper.[14] The present apparatus is essentially identical to that given in Ref. 14 with the solid-state detector replaced by an electrostatic differential velocity analyzer of the Mollenstedt type[15] which had an optimum resolution of at least 1.5×10^{-5} [0.4 eV full width at half-maximum (FWHM)/25 keV]. An incident electron beam intensity of 200 μA obtained from a telefocus electron gun[16] with a diameter of 400-μ FWHM was allowed to impinge at a right angle on a gas jet with a nozzle diameter of 125 μ, and a flow rate of 1.6×10^{20} He atoms per second. The optimum vacuum of the scattering chamber, which had a pumping speed of about 15000 liter/sec, was 3×10^{-7} torr and increased to 4×10^{-5} torr during an experiment,